48th AIAA/ASME/ASCE/AHS/ASC Structures, Structural Dynamics, and Materials Conference
23 - 26 April 2007, Honolulu, Hawaii

AIAA 2007-2004

Experimental and Numerical Analysis of a DECSMAR Structure's Deployment and Deployed Performance

Eric L Pollard*
CSA Engineering, Inc., Albuquerque, NM 87123-3831 US

Thomas W Murphey†
Air Force Research Laboratory, Albuquerque, NM, 87117-5776 US

&
Gregory E Sanford‡
CSA Engineering, Inc., Albuquerque, NM 87123-3831 US

The objective of this research is to analyze the deployment and deployed performance of a recently developed, self-deployable truss architecture composed of carbon fiber reinforced plastic (CFRP) tape-spring elements and embedded shape memory alloy (SMA) flexures; this particular structural system is referred to as deployable elastic composite shape memory alloy reinforced (DECSMAR) and is representative of a concentrated, material deformation based deployable architecture. The scope of this study encompasses numerically and experimentally mapping the force profile through the deployment path of a 450 mm radius DECSMAR boom and then to numerically determine the effective continuum, deployed stiffness and strength properties, i.e., bending, shear, torsion, and axial moduli with corresponding critical loads, correlated to experimental analysis, of an equivalent radius, five-bay DECSMAR boom. Minimum deployment force to linear mass and bending modulus to linear mass ratios were measured at 2.79 $Nmkg^{-1}$ and 2.38 MNm^3kg^{-1}, respectively. Of particular interest were deleterious effects of the deployment sequencer on the force profile, the deployed performance attributable to the SMA flexure features, and consequences of flattening longeron ends to buy packaging efficiency. Developmental aspects of the DECSMAR architecture, including the design space of the individual CFRP tape-spring element, an exercise for a point design of a 180 mm radius DECSMAR boom with correlation to experimental analysis, and performance implications of scaling the truss radius, are focused on in a prequel manuscript.

I. Introduction

SELF-DEPLOYALBE structures, designed to exploit mass, volume, and power otherwise allocated to attendant deployment mechanisms, can be mission enhancing or can be even enabling solutions when actively deployed space platform counterparts exceed launch vehicle and bus accommodations. Architectures with the capacity to store and capability to harness potential strain energy to motivate reconfiguration between stowed and operational states customarily exhibit deployment force profiles with lower minimums than active alternatives; their utility can pivot on this metric. With less margin to overcome unanticipated non-conservative phenomena encountered during reconfiguration events, high fidelity deployment predictions with empirical credence to optimize the force profile and survey kinematic paths to judge deployment destiny will prove an invaluable tool. Additionally, more comprehensive effective stiffness and strength-stability property experimental evaluations and parallel modeling

* Engineer, CSA Engineering, Inc., 1451 Innovation Pkwy. SE Suite 100, Albuquerque, NM 87123-3831 US, AIAA Member
† Research Aerospace Engineer, Space Vehicles Directorate, 3550 Aberdeen Ave. SE, Albuquerque, NM 87117-5776 US, AIAA Senior Member
‡ Project Engineer, CSA Engineering, Inc., 1451 Innovation Pkwy. SE Suite 100, Albuquerque, NM 87123-3831 US, AIAA Member

Report Documentation Page

Form Approved
OMB No. 0704-0188

1. REPORT DATE	2. REPORT TYPE	3. DATES COVERED
APR 2007		**00-00-2007 to 00-00-2007**

4. TITLE AND SUBTITLE	5a. CONTRACT NUMBER
Experimental and Numerical Analysis of a DECSMAR Structure's Deployment and Deployed Performance	5b. GRANT NUMBER
	5c. PROGRAM ELEMENT NUMBER
6. AUTHOR(S)	5d. PROJECT NUMBER
	5e. TASK NUMBER
	5f. WORK UNIT NUMBER
7. PERFORMING ORGANIZATION NAME(S) AND ADDRESS(ES) **Air Force Research Laboratory,Space Vehicles Directorate,3550 Aberdeen Ave. SE,Albuquerque,NM,87117-5776**	8. PERFORMING ORGANIZATION REPORT NUMBER
9. SPONSORING/MONITORING AGENCY NAME(S) AND ADDRESS(ES)	10. SPONSOR/MONITOR'S ACRONYM(S)
	11. SPONSOR/MONITOR'S REPORT NUMBER(S)

12. DISTRIBUTION/AVAILABILITY STATEMENT
Approved for public release; distribution unlimited

13. SUPPLEMENTARY NOTES
48th AIAA/ASME/ASCE/AHS/ASC Structures, Structural Dynamics, and Materials Conference, 23 - 26 April 2007, Honolulu, Hawaii

14. ABSTRACT

15. SUBJECT TERMS

16. SECURITY CLASSIFICATION OF:			17. LIMITATION OF ABSTRACT	18. NUMBER OF PAGES	19a. NAME OF RESPONSIBLE PERSON
a. REPORT **unclassified**	b. ABSTRACT **unclassified**	c. THIS PAGE **unclassified**	**Same as Report (SAR)**	**16**	

predictions of deployable structures to strategically allocate system structural and control requirements will reduce risk for lean deployed performance margin applications.

A. Concept

The deployable elastic composite shape memory alloy reinforced (DECSMAR) truss concept is a recently developed, self-deployable truss architecture composed of carbon fiber reinforced plastic (CFRP) tape-spring elements and embedded shape memory alloy (SMA) flexures.[1] The non-prismatic longerons have traverse reduced thickness gauge sections to enable equal and opposite sense bending where the length of the reduced thickness regions corresponds to the radius of the fold and pi. Consequently, the thickness and length of the hinge region or the distance from the neutral-plane and the bend radius dictate the strain realized. In order to minimize the bend radius for increased compaction efficiency, a less structurally efficient and more compliant material system is utilized for the hinge regions while a more efficient and less compliant material system is utilized throughout the majority of the structure. It may not be intuitive this pairing of structural roles leads to greater mass efficiency as well. These monolithic hinges are deliberately placed to enforce packaging kinematics; longerons z-fold and the battens torque and nest (Fig. 1). To mitigate the compromise of deployed performance due to the hinge cross-section, Nitinol SMA wires can be embedded in the composite lay-up across the reduced thickness region. Thicker wires of binary NiTi can accommodate the same radius as the thinner CRFP through superelastic deformation.

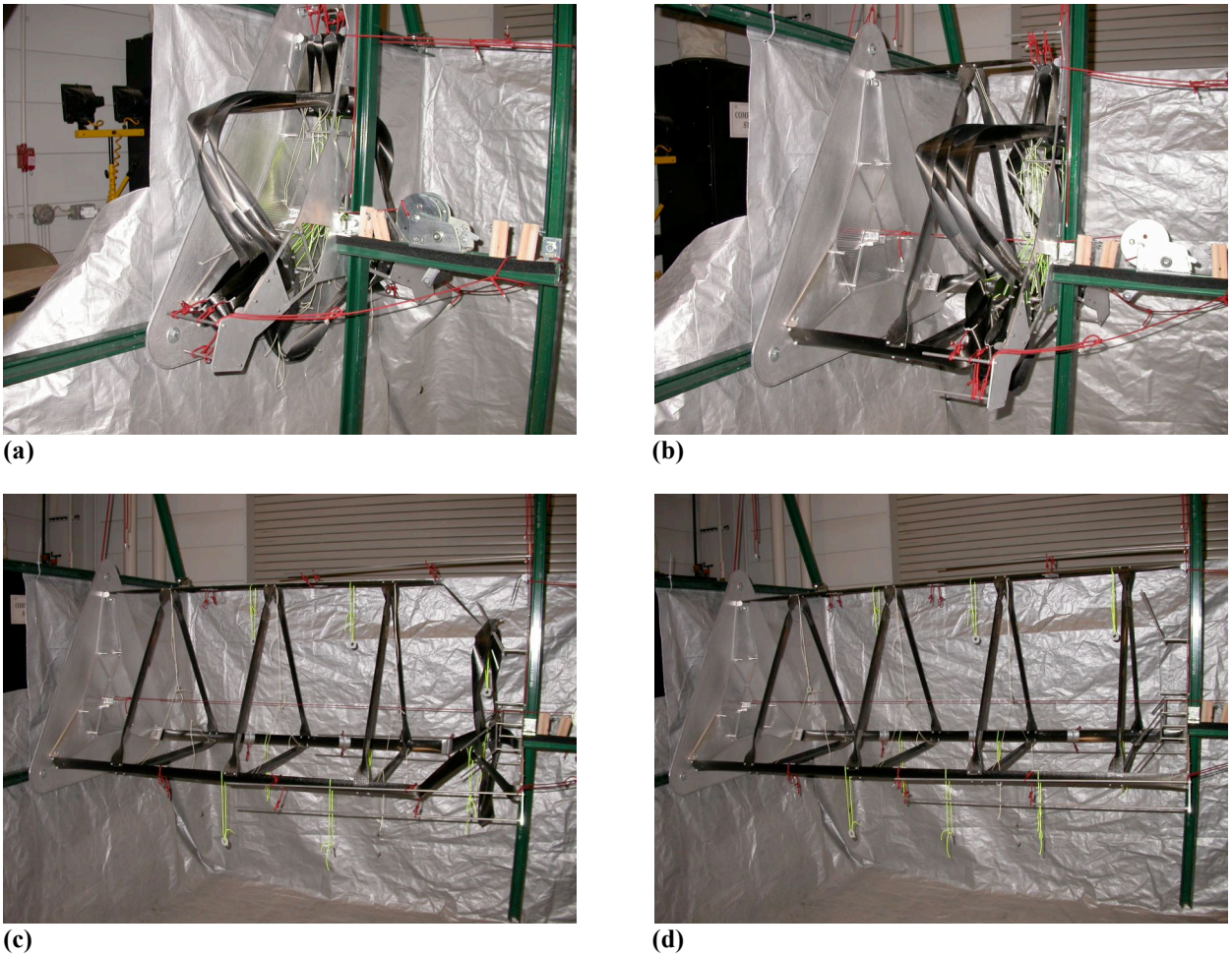

Fig. 1 Four-bay DECSMAR boom prototype with nesting battens and passive deployment sequencer shown as, (a) packaged configuration; (b) first bay deployed and tethers to trigger second bay retainers; (c) fourth bay to deploy along guides; (d) and deployed configuration.

Again, battens must have the ability to nest in order to realize the longeron strain limited bay packaged length. The design for this transverse member, which accommodates the aforementioned kinematics, was virtually prototyped, iteratively modifying and analyzing concepts with 3D modeling and finite element (FE) tools. This effort resulted in a series of quadratic cross-section transitions and is notable as the bending neutral planes of the cross-sections are coaxial to avoid inherent eccentricity.

Additionally, a compatible, passive deployment sequencer can be integrated into a DECSMAR system. This mechanism, as visible in Fig. 1, is composed of (i) retainers to prevent packaged bays, tethered at opposite sense hinges to a mast along the boom's primary structural axis, from releasing until triggered by the deployment of a preceding bay, via a second set of tethers, (ii) guides extending from the retainers to limit premature deployment of longerons and battens, and (iii) guides interfacing with the structure at equal sense hinges along each longeron to reconcile the orientation of the packaged and transition segments to deployed structure to autonomously index deploying events in a bay-by-bay progression of a DECSMAR like deployable architecture which reconfigures through bending about alternating sense transverse axes indexed along the length of the longitudinal members. The sequencer is motivated by the stored strain energy of the resiliently folded structure.

B. Background

Deployable structures customarily require some attendant system with authority over sequence and rate to reconfigure between stowed and operational states. For space applications, active mechanisms expend significant mass and volume budgets relative to the packaged structure and active deployment consumes considerable power resources relative to other spacecraft demands. Prior art has focused on active systems with devices to acquire the deployed configuration of an architecture in a piece-wise progression[2] and active systems with means to inflate and rigidize members of an architecture either sequentially or synchronously.[3] Although passive deployment schemes are more desirable as they are more efficient, they are higher risk and limited concepts have demonstrated feasibility to exploit the stored strain energy or other potential to sequence and rate control deployment events.[4] Additionally, there are limited documented efforts in the literature to thoroughly experimentally investigate deployable structures suited for the class of expected loads and requirements Hedgepeth[5] describes. Some notable examples locate points of fidelity within the design space which can drift from theoretical expectations.[6-8]

C. Objective

The objective of this research is to analyze the deployment and deployed performance of the DECSMAR truss concept, a concentrated, material deformation based deployable architecture. The scope of this study encompasses numerically and experimentally mapping the force profile through the deployment path of a 450 mm radius DECSMAR boom and then to numerically determine the effective continuum, deployed stiffness and strength properties, i.e., bending, shear, torsion, and axial moduli with corresponding critical loads, correlated to experimental analysis, of an equivalent radius, five-bay DECSMAR boom. Of particular interest were deleterious effects of the deployment sequencer on the force profile, the deployed performance attributable to the SMA flexure features, and consequences of flattening longeron ends to buy packaging efficiency.

II. Deployment Performance Analysis

A. Model

Predictions of the deployment force profile developed by the 450 mm radius, 30.0° diagonal angle, and three-longeron DECSMAR test article were conducted with a one-third symmetry, numerical model of substantially a single bay. Figure 2 depicts the FE model with parting lines indicating unique laminates such as the three 30.0 mm length longeron hinges and the 114 mm length batten transition loft, 25.4 mm length collar, then axially prismatic sections (Table 1). Consistent with the test article baseline design, the model was not SMA reinforced. This modeled article is capable of 4.24% linear compaction ratio realizing 1.57% maximum strain. To ensure the representative boundaries of the deployment transition zone were captured, the longerons of the FE model were extended 113 mm, or half-way to the center of the next hinge, at either extreme beyond the length of a single-bay; rigid body conditions were assumed at each 120° subtended, 28.6 mm radius longeron face. Plane symmetry boundaries were enforced on the 150° subtended, 19.1 mm radius batten cross-section faces. Full-integration shell elements assumed to have linear moment-bending and force-membrane strain relationships assigned with composite section definitions represented the various laminates throughout the FE model at a global seed size of 2.00 mm and lamina material constants were consistent with experimental results of the IM7/977-2 system.[9] The ABAQUS Standard finite element code's non-linear static solver was employed to determine the displaced solutions.[10]

Fig. 2 One-third symmetry, numerical model of substantially a single bay.

Table 1 Unique laminates such as the three 30.0 mm length longeron hinges and the 114 mm length batten transition loft, 25.4 mm length collar, than axially prismatic sections.

Laminate	Lamina	Material	Thickness	Orientation
longeron	1	IM7/977-2	100 μm	0˚
	2	IM7/977-2	200 μm	±45˚
	3	IM7/977-2	100 μm	0˚
longeron hinge	1	IM7/977-2	100 μm	0˚
	2	IM7/977-2	100 μm	0˚
SMA reinforced longeron hinge	1	IM7/977-2	100 μm	0˚
	2 (two, 1.47 mm width wires positioned along longitudinal edges)	Nitinol	305 μm	N/A
	3	IM7/977-2	100 μm	0˚
batten transition	1	IM7/977-2	200 μm	±45˚
	2	IM7/977-2	200 μm	±45˚
batten collar	1	IM7/977-2	200 μm	±45˚
	2	IM7/977-2	100 μm	0˚
	3	IM7/977-2	100 μm	0˚
	4	IM7/977-2	200 μm	±45˚
batten	1	IM7/977-2	100 μm	0˚
	2	IM7/977-2	100 μm	90˚
	3	IM7/977-2	100 μm	0˚

A suite of essential and natural boundary conditions were activated and deactivated through a series of analysis steps, stabilized by invoking the ABAQUS dissipated energy functionality, to reconfigure the symmetry model to a packaged state. This configuration is quantified by a 528 mm collapse of the two reference points, representing the rigid cross-section faces of the longeron, along the second axis (Fig. 3). Once packaged, the relative position between the two reaction nodes, corresponding to complete deployment of the bay, was proportionally sought. This progression was interrupted at intervals and a final sequence of steps were appended to wean the solutions from stabilization and allow the FE model to acquiesce. The reaction force acting parallel to the second axis, the primary structural axis, was then logged. The kinematic constraints of the sequencer guides were not honored and contact friction was not modeled; disagreement between predicted and measured profiles was expected to be attributable to effects of the deployment sequencer.

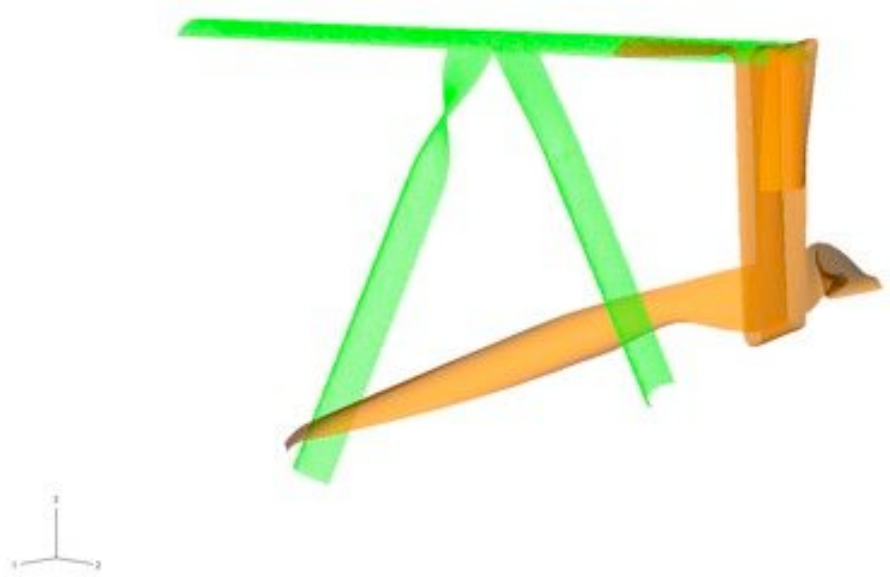

Fig. 3 A suite of essential and natural boundary conditions were activated and deactivated through a series of analysis steps, stabilized by invoking the ABAQUS dissipated energy functionality, to reconfigure the symmetry model to a packaged state.

B. Test Setup

Measurement of the deployment force profile, developed by the passively sequenced, 450 mm radius, 30.0° diagonal angle, and three-longeron DECSMAR test article, was sought by fixedly attaching a 1.33 kN capacity load cell, rated at 0.08% full scale precision, to the out-board endplate of the boom. The article was mounted normal to gravity at the in-board endplate and the load cell, out-board endplate, and cantilevered structure were off-loaded from a trolley constrained to a track parallel to the primary structural axis (Fig. 4). A single bay was folded, consistent with the packaged state of the FE analysis, then the bay was payed out at 2.54 mms^{-1} with a linear actuator, which had a 0.25% over 76.2 mm precision displacement channel, via a tether acting through the load cell. The tether tensile load was recorded against extension. To negate influence of the off-load boundary on the measured profile, the trolley was simultaneously actuated via a second tether to ensure the off-load point kept station above the out-board endplate.

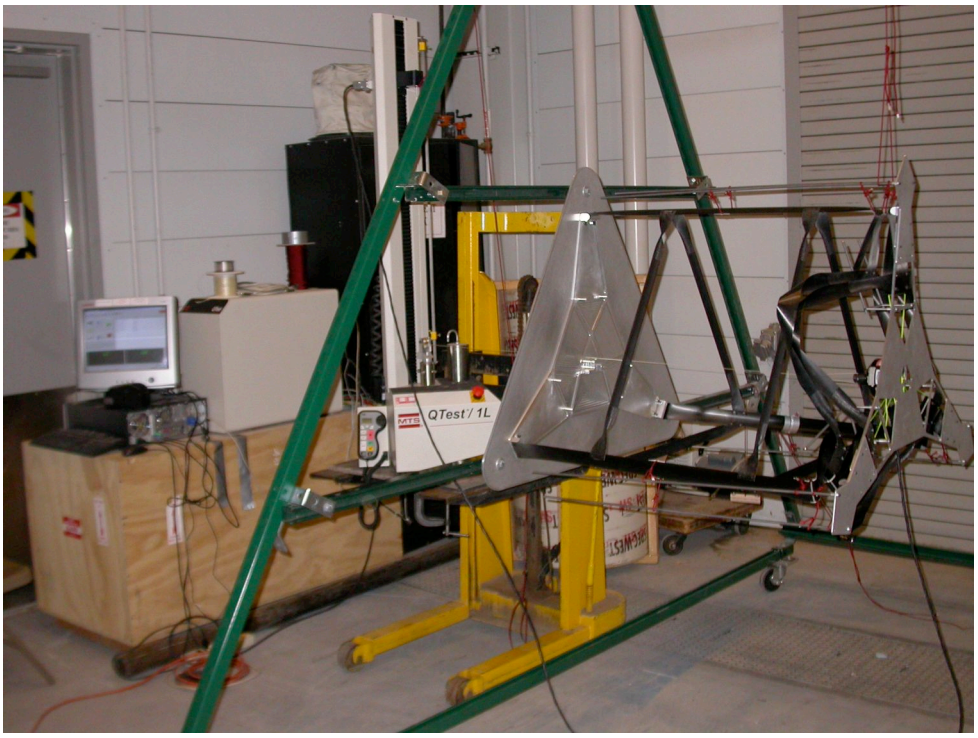

Fig. 4 Measurement of the deployment force profile, developed by the passively sequenced, 450 mm radius, 30.0˚ diagonal angle, and three-longeron DECSMAR test article, was sought by fixedly attaching a 1.33 kN capacity load cell, rated at 0.08% full scale precision, to the out-board endplate of the boom. The article was mounted normal to gravity at the in-board endplate and the load cell, out-board endplate, and cantilevered structure were off-loaded from a trolley constrained to a track parallel to the primary structural axis.

C. Results

The predicted deployment force profile of the one-third symmetry, FE model of substantially a single bay maps a notional strain energy release through a single bay reconfiguration (Fig. 5). Figure 6 illustrates the model's kinematic path corresponding to logged points plotted in Fig. 5. The measured deployment force profile developed by the 450 mm radius, 30.0˚ diagonal angle, and three-longeron DECSMAR test article follows a similar trend with the greatest energy available upon stabilizing the battens. Interestingly, the anomaly at approximately 280 mm extension was the result of the experimentally observed premature deployment of the lower batten as is evident from Fig. 6m. Final conditions of each profile are not representative of a continuously cyclic, sequenced deployment as both were effectively interrupted. The experimental run was arrested because the sequencer triggers to release the last bay were not set and consequently its expected contribution to the measured reaction was not realized; these triggers are timed to trip coincident with batten stabilization. The numerical run was interrupted because the subsequent bay was not modeled and consequently its strain energy was not captured. Final conditions would be expected to cycle back to the initial condition force values.

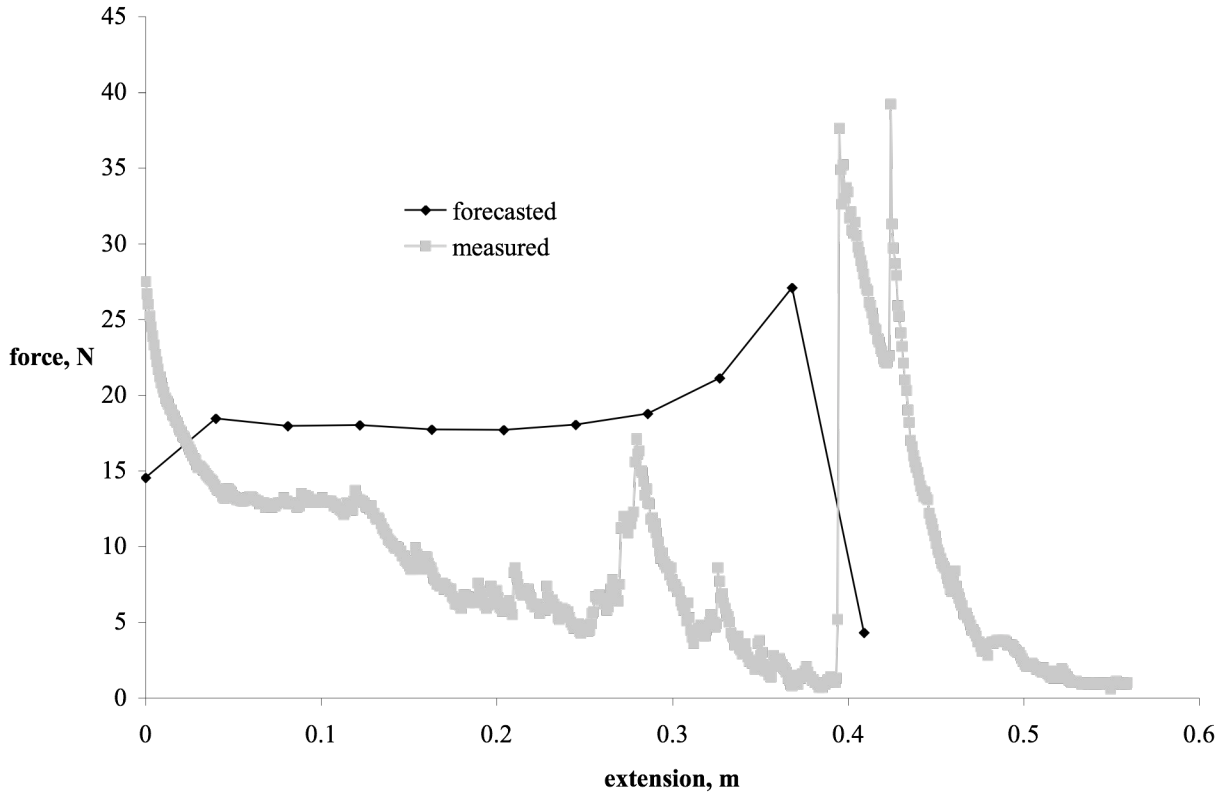

Fig. 5 The predicted deployment force profile of the one-third symmetry, FE model of substantially a single bay maps a notional strain energy release through a single bay reconfiguration. The measured deployment force profile developed by the 450 mm radius, 30.0° diagonal angle, and three-longeron DECSMAR test article follows a similar trend with the greatest energy available upon stabilizing the battens.

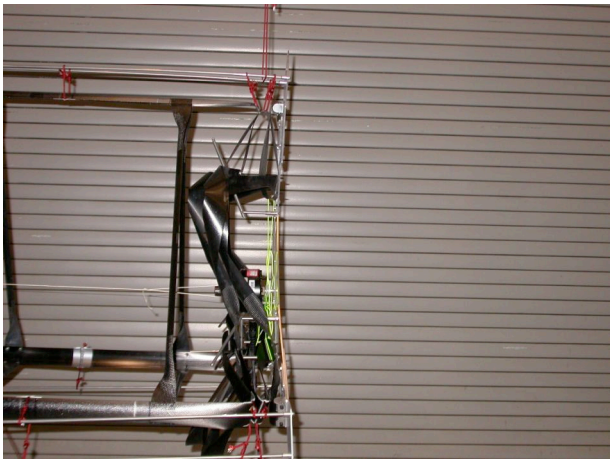

(a)

(b)

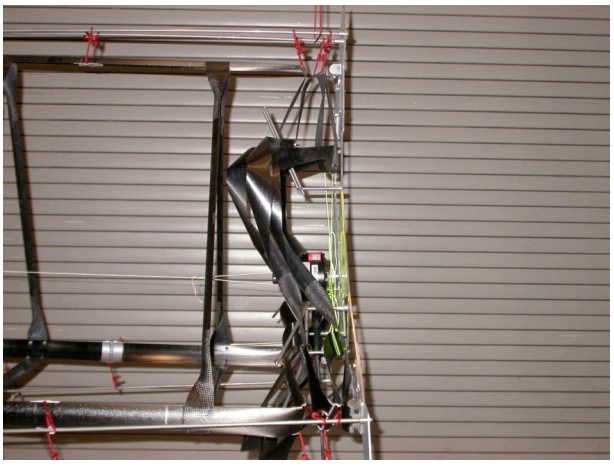

(c)

(d)

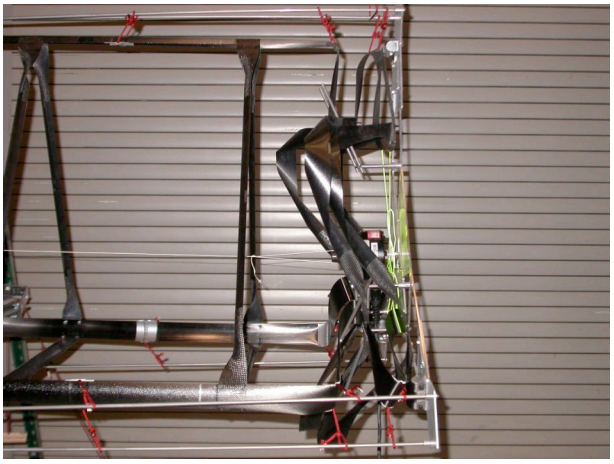

(e)

(f)

(g)

(h)

(i)

(j)

(k)

(l)

(m)

(n)

(o)

(p)

(q)

(r)

(s)

(t)

(u)

(v)

Fig. 6 Experimentally observed and modeled kinematic path through the deployment event sequence of a 450 mm radius, 30.0° diagonal angle, and three-longeron DECSMAR test article and one-third symmetry, FE model of substantially a single bay.

D. Error Analysis

Instrumentation confidence intervals can be determined for this investigation based on the appropriate load cell and displacement sensor ratings. Load cell precision was conservatively taken as the summation of static error band and non-linearity contributors. Considering the instrument ratings as they pertain to the deployment run, measured extension errors could have accumulated to as much as 1.40 mm and measured force can be certain within ±1.06 N.

III. Deployed Performance Analysis

A. Model

FE predictions of the effective continuum stiffness and strength-stability properties exhibited by a fixed-free supported unreduced five-bay DECSMAR boom, comparable to the test article, were made with the same modeling parameters as the deployment force profile investigation (Fig. 7a). In order to illustrate the merit of incorporating the SMA flexure features into the hinges, solutions were found without and with this enhancement. (To serve as a baseline design, the test article was not SMA reinforced.) The resiliency of this 2.31 m and 580 g truss was identified employing the ABAQUS Standard finite element code's static solver and negative pivot loads were determined employing the ABAQUS Standard finite element code's subspace eigensolver.[9] Rigid endplate boundary conditions were emulated by defining two-rigid bodies on the boom's axis at either end with which each respective set of longeron faces participates. Geometric stiffness is not leveraged at these flattened extremes; longeron faces are rectilinear, transitioning from the tape-spring cross-section which characterizes the majority of their length. These transitions enable hinge placement at the endplates, enhancing packaging efficiency, but also compromising shear stiffness and member axial stability. To quantify this trade, a FE model with arcuate longeron ends was also studied.

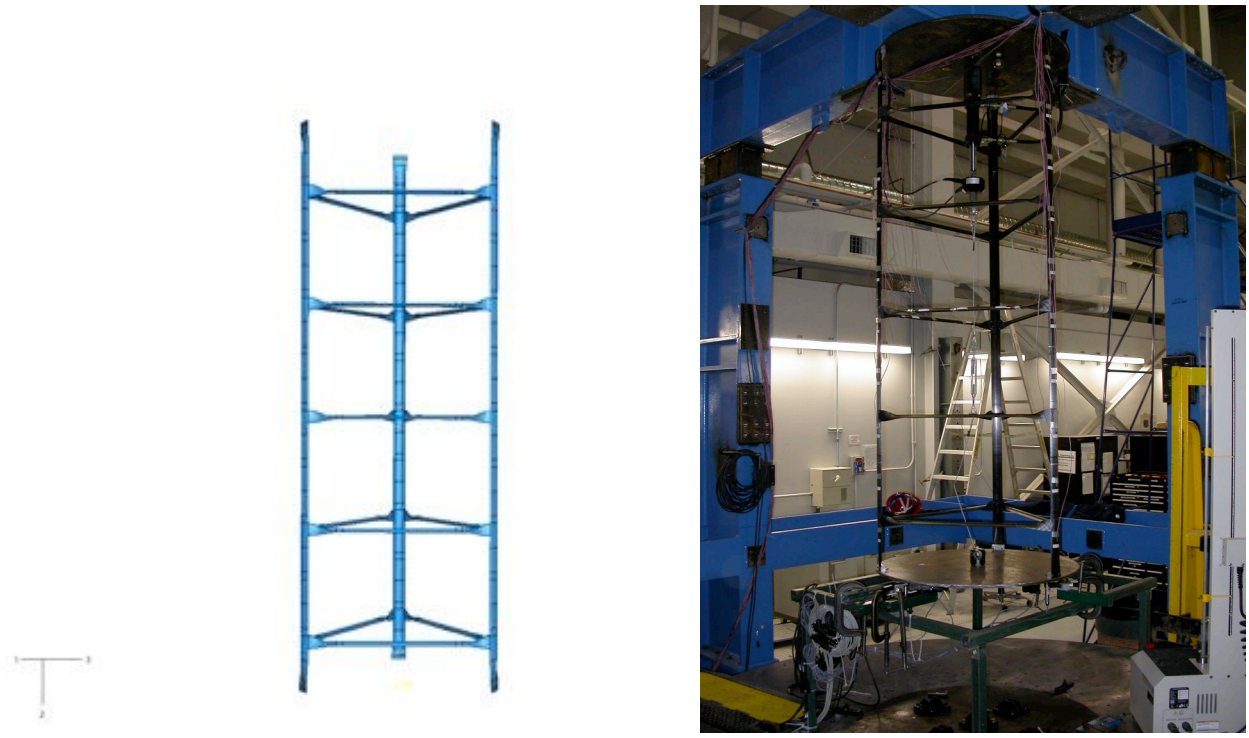

(a) (b)

Fig. 7 (a) FE predictions of the effective continuum stiffness and strength-stability properties exhibited by a fixed-free supported unreduced five-bay DECSMAR boom, comparable to the test article, were made with the same modeling parameters as the deployment force profile investigation. (b) Experimental evaluation of the five-bay DECSMAR test article followed encastre mounting the top of the truss, oriented parallel to gravity, to a reaction structure and fixedly attaching a plate at the opposing free end to serve as a proxy for the modeled rigid body and to accommodate various actuator and sensor configurations to affect and measure the article.

B. Test Setup

Experimental evaluation of the five-bay DECSMAR test article followed encastre mounting the truss, oriented parallel to gravity, to a reaction structure and fixedly attaching a plate at the opposing free end to serve as a proxy for the modeled rigid body and to accommodate various actuator and sensor configurations to affect and measure the article (Fig. 7b). The free end plate was off-loaded with an active tether at its center of gravity for all load cases; this tether was servo-hydraulically load controlled with a 7.12 kN actuator and a 1.33 kN capacity load cell rated at 0.08% full scale precision. An array of 12.7 mm range linear variable displacement transducers, rated at 0.35% full scale non-linearity, oriented parallel and transverse to the boom's primary structural axis, probed the plate to detect compliance. Transversely oriented transducers were paired with an opposing dead channel transducer to negate the influence of the probes' 2.45 N preload. Both longerons and battens were populated with strain gauges at varying linear frequencies to investigate loading symmetry and transverse member densities to perceive moment communication load path allocation.

Bending load cases were performed with an additional pair of servo-hydraulically load controlled assemblies, with identical actuators to the off-load channel, but mated to 8.90 kN capacity load cells rated at 0.08% full scale precision. These assemblies were pinned-pinned mounted between the free end plate and the base of the reaction structure to form a symmetric couple about the article's geometric center at a 305 mm radius. Shear and torsion load cases were performed with the same linear actuator as employed for the deployment force profile investigation via a tether acting normal to gravity and through a 97.9 N capacity load cell, rated at 0.08% full scale precision, to the free end plate center and at a 229 mm radius or moment arm from the center, respectively. Axial load cases were

performed with the active off-load channel. The bending and torsion load case configurations relied on laser sight located actuator and end plate mounts to vertically align the boom, whereas the axial and shear load case configuration did not include a vertical alignment design element at the free end. A free axle disposed between the base of the reaction structure and the free end plate center served as such element for the torsion load cases. Loads were engaged incrementally with sine waveform step profiles.

C. Results

Agreement between the experimentally evaluated, effective continuum stiffness and strength-stability properties exhibited by the fixed-free supported five-bay DECSMAR boom test article and FE predictions vary by load case between 4.3% and 33.7% for compliance and between 6.9% and 53.3% for elastic stability (Tables 2 and 3). Bending force was assumed as the average of the two load cell channels; transverse displacement values used to calculate the reported compliances were taken as the average value of two live transducers located near the perimeter of the free end plate and 180° apart. A discussion on the corrections made for the off-load restoring force follows. Complications with vertical alignment of the test article invalidated the axial load cases. Interrogation of the strain gauge channels were indicative of the loading symmetry which averaged 37.5 % discrepancy between the two tensile loaded longerons during the bending compliance test and revealed indistinguishable shear across the batten elements unlike the more frame-like structure considered in Ref. 1. Beyond the quantified improvement in the bending load case first negative pivot of the FE model with arcuate longeron ends relative to the baseline FE model, the former responded with a different mode shape; both the test article and FE model buckled at the flattened longeron extremes, where as the FE model with arcuate longeron ends shed load by destabilizing along the interior of the longeron length.

Table 2 Effective continuum stiffness properties as predicted with FE models and evaluated experimentally.

Property	FE Model	Test Article	SMA Reinforced FE Model	FE Model with Arcuate Longeron Ends
bending modulus	598 kNm^2	665 kNm^2	633 kNm^2	693 kNm^2
shear modulus	1.65 kN	2.49 kN*	1.66 kN	2.20 kN
torsion modulus	651 Nm^2	680 Nm^2	657 Nm^2	827 Nm^2
axial modulus	6.21 MN		6.24 MN	7.08 MN
	*corrected for off-load restoring force			

Table 3 Effective continuum strength-stability properties as predicted with FE models and evaluated experimentally.

Property	FE Model	Test Article	SMA Reinforced FE Model	FE Model with Arcuate Longeron Ends
bending strength	105 Nm	98.2 Nm	127 Nm	188 Nm
shear strength	4.58 N	3.87 N*	5.43 N	7.50 N
torsion strength	3.68 Nm	2.40 Nm	4.28 Nm	6.46 Nm
axial strength	458 N		507 N	715 N
	*corrected for off-load restoring force			

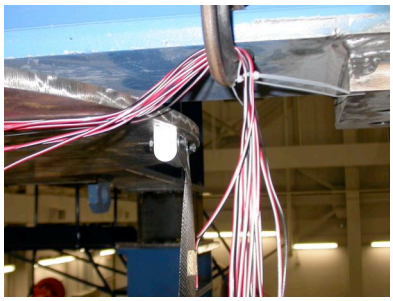

(a)

(b)

(c)

Fig. 8 Experimentally observed bending, buckling mode of the five-bay DECSMAR test article, (a) at top of the longeron; (b) and at base of the longeron. (c) FE modeled bending, buckling mode of the unreduced five-bay DECSMAR boom with arcuate longeron ends.

D. Error Analysis

Instrumentation confidence intervals can be determined for this investigation based on the appropriate load cell and displacement sensor ratings. Load cell precision was taken as the summation of static error band and non-linearity contributors. Confidence intervals, expressed in the corresponding property dimensions, were figured for each load case conservatively assuming load cell precision extremes and worst-case transducer non-linearity accumulation was realized over the data considered for identification. The shear stiffness confidence interval is not compounded by bending stiffness uncertainty (Table 4).

Table 4 Confidence intervals, expressed in the corresponding property dimensions, were figured for each load case.

Property	Bending	Shear	Torsion	Axial
stiffness	±195 kNm^2	±202 N	±26.1 Nm^2	N/A
strength	±4.34 Nm	±78.3 mN	±17.9 mNm	N/A

Corrections must be made in the recorded force for the shear load cases to account for the off-load restoring force. This measurement contamination arises as the test article's free end is displaced off vertical center and the off-load channel, commanded to maintain the weight force of the free end plate at 658 N, projects a force component in a direction transverse to the boom's primary structural axis (Fig. 9). Transverse force data was post processed to remove the contamination.

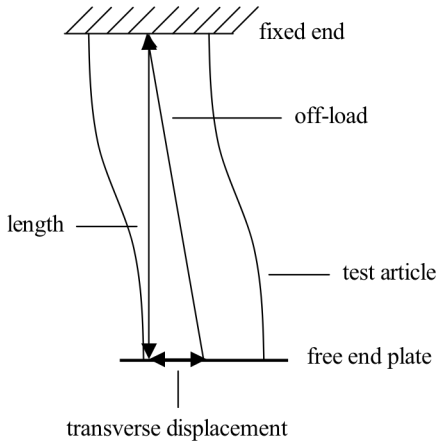

Fig. 9 Corrections must be made in the recorded force for the shear load cases to account for the off-load restoring force.

IV. Discussion

This research analyzed the deployment and deployed performance of a recently developed. self-deployable truss architecture composed of CFRP tape-spring elements and embedded SMA flexures; this particular structural system is referred to as DECSMAR and is representative of a concentrated, material deformation based deployable architecture. The scope of this study encompassed numerically and experimentally mapping the force profile through the deployment path of a 450 mm radius DECSMAR boom. Minimum deployment force to linear mass ratio was measured at 2.79 Nmkg. Although the deployment sequencer demonstrated robustness, as the experimental run recovered from a premature batten deployment, non-conservative deleterious effects of the mechanism on the force profile were found to be significant against the predicted strain energy release.

The scope of this study also included numerically determining the effective continuum, deployed stiffness and strength properties, i.e., bending, shear, torsion, and axial moduli with corresponding critical loads, correlated to experimental analysis, of an equivalent radius, five-bay DECSMAR boom. Bending modulus to linear mass ratio was measured at 2.38 MNm^3kg^{-1}. Although the experimentally evaluated effective continuum strength-stability properties compare reasonably well with predicted values, instrumentation confidence intervals and off-load restoring force contamination combined do not provide a complete explanation for the test article generally outperforming the stiffness of a theoretical, numerical model. Suspected as aliasing the true structural response are extraneous constraints inherently imposed when affecting the article, i.e., the pair of servo-hydraulically load controlled assemblies forming a couple for the bending load cases can pivot and piston, but not follow the free-end to the fidelity of a pure moment applied to the FE model. Another suspect perhaps culpable for aliasing the true structural response is the loss of off-load as the structure deflects transversely, effectively pre-loading the article, i.e., the complimentary projection of the off-load force onto the gravity vector of the free end plate decreases as the off-load restoring force increases. Performance attributable to the SMA flexures was more pronounced over the baseline strength values and can be quantified per the mass penalty through the bending modulus linear mass efficiency metric which distills to 2.50 MNm^3kg^{-1}. The consequence of flattening longeron ends to buy packaging efficiency is not insignificant and alters the nature of the buckling mode response; this penalty trades well with increasing length as it does not scale proportional to additional bays.

Acknowledgments

Funding for this research was provided by the Air Force Research Laboratory Space Vehicles Directorate and monitored by Dr. Jeffry S Welsh. The authors are grateful for the expertise and support of the directorate's modeling and composites laboratories.

References

[1]Pollard, EL & Murphey, TW, "Development of Deployable Elastic Composite Shape Memory Alloy Reinforced (DECSMAR) Structures," *Proceedings of the 47th AIAA/ASME/ASCE/AHS/ASC Structures, Structural Dynamics, & Materials Conference*, 2006-1681, AIAA, Washington, DC, US, 2006.

[2]Warden, RM & Jones, PA, "Carousel Deployment Mechanism for Coilable Lattice Truss," *Proceedings of the 23rd Aerospace Mechanisms Symposium*, 1989, pp. 77-100.

[3]Freeland, RE, Bilyeu, GD, Veal, GR, & Mikulas, MM, "Inflatable Deployable Space Structures Technology Summary", 98-I.5.01, IAF, Cedex, France, 1998.

[4]"Boom Deploys with Controlled Energy Release," NASA Tech Brief, Vol. 7, No. 2, Item 36, 1982.

[5]Hedgepeth, JM, "Critical Requirements for the Design of Large Space Structures," NASA CR-3484, 1981.

[6]Crawford, RF, "Investigation of a Coilable Lattice Column," NASA CR-1301, 1969.

[7]Hinkle, JD, Warren, P, & Peterson, LD, "Structural Performance of a Gossamer Isogrid Column with Initial Geometric Imperfections," *Proceedings of the 42nd AIAA/ASME/ASCE/AHS/ASC Structures, Structural Dynamics, & Materials Conference*, 2001-1682, AIAA, Washington, DC, US, 2001.

[8]Hinkle, JD, Peterson, LD, & Warren, PA, "Structural Performance of an Elastically Stowable Tubular Truss Column," *Proceedings of the 43rd AIAA/ASME/ASCE/AHS/ASC Structures, Structural Dynamics, & Materials Conference*, 2002-1555, AIAA, Washington, DC, US, 2002.

[9]Welsh, JS & Wegner, PM, "The Effect of Adhesive Bond Thickness and Material Type on Structure Stiffness," *Proceedings of the 43rd AIAA/ASME/ASCE/AHS/ASC Structures, Structural Dynamics, and Materials Conference*, 2002-1726, AIAA, Washington, DC, 2002.

[10]*ABAQUS/Standard User's Manual*, Hibbitt, Karlsson, & Sorensen, Inc., 2006.